# Fragmentation of drying paint layers

Katinka Bakos, András Dombi, Ferenc Járai-Szabó, and Zoltán Néda

Citation: AIP Conference Proceedings **1564**, 205 (2013); doi: 10.1063/1.4832819
View online: http://dx.doi.org/10.1063/1.4832819
View Table of Contents: http://scitation.aip.org/content/aip/proceeding/aipcp/1564?ver=pdfcov
Published by the AIP Publishing

# Fragmentation of Drying Paint Layers

Katinka Bakos, András Dombi, Ferenc Járai-Szabó and Zoltán Néda

*Faculty of Physics, Babeș-Bolyai University,*

*Str. Kogălniceanu 1, RO–400080, Cluj–Napoca, Romania*

**ABSTRACT.** Fragmentation of thin layers of drying granular materials on a frictional surface are studied both by experiments and computer simulations. Besides a qualitative description of the fragmentation phenomenon, the dependence of the average fragment size as a function of the layer thickness is thoroughly investigated. Experiments are done using a special nail polish, which forms characteristic crack structures during drying. In order to control the layer thickness, we diluted the nail polish in acetone and evaporated in a controlled manner different volumes of this solution on glass surfaces. During the evaporation process we managed to get an instable paint layer, which formed cracks as it dried out. In order to understand the obtained structures a previously developed spring-block model was implemented in a three-dimensional version. The experimental and simulation results proved to be in excellent qualitative and quantitative agreement. An earlier suggested scaling relation between the average fragment size and the layer thickness is reconfirmed.

**Keywords:** spring-block model, crack formation, crack propagation.

## I. INTRODUCTION

Fragmentation of solid materials is a common phenomenon in nature. Fragmentation patterns or cracked structures are often observable on dried out fields, battered roads, dried coffee grounds and other granular materials. Moreover, the durability of most products is strongly related to its fracture mechanical behavior. Cracks are also present in our technical products on both macroscopic and microscopic scales. Since the durability of most products is related with their fracture resistance, the problem of fracture and fragmentation presents practical interest. In such contexts the crack propagation phenomenon was widely investigated [1], and it is still subject of both large scientific and industrial studies [1-8].

Recent theoretical and simulation studies proved that a discrete spring-block model can elegantly reproduce the main qualitative and topological features of the cracks and some experimentally observed scaling laws for the fragment-size statistics [9, 10]. The same model-family was successfully applied for studying crack propagation in glass plates [11] and spiral crack formation in drying precipitates [12]. Moreover, the spring-block model applied at the nanoscale level explained the self-organized structures obtained in drying nanosphere systems on glass surfaces [13]. Up to now, the majority of the spring-block type simulations were realized in quasi-three-dimensional approach. In order to obtain a computationally efficient model, the thickness of the material has been forced in a two-dimensional spring-block topology, where the blocks are allowed to move on the surface of a two dimensional plane and the third dimension (thickness) is taken into account by using multiple spring layers between the blocks [9,10].

In the present study we continue to develop the spring-block type approach for crack formation and propagation in drying granular materials, considering a three-dimensional version of the model. The thickness of the granular material will be taken into account in a more realistic manner, by considering a three-dimensional array of springs and blocks. The fragmentation patterns modeled in such a manner are compared with the structures experimentally observed in thin drying paint layers. In order to go beyond a pure qualitative visual comparison, the characteristic scaling of the average fragment size as a function of the layer thickness is also studied.

The paper is organized as follows. In the next section the experimental procedure and results are detailed. In Section III the used spring-block model is described, and in section IV the obtained experimental and simulation results are discussed. Section V contains our brief conclusions and further outlook.

*TIM 2012 Physics Conference*
AIP Conf. Proc. 1564, 205-210 (2013); doi: 10.1063/1.4832819

## II. EXPERIMENTAL RESULTS

In order to produce fragmented layers of granular materials with controlled thicknesses, a special nail polish has been used. This cosmetic product seems to be very trendy nowadays because it forms characteristic crack-patterns as it dries out. The nail polish has been diluted in acetone and different amounts of this solution were poured in graded plastic tubes that were glued on a horizontally fixed glass surface. As the acetone evaporates at the open end of the tube, a wet granular layer forms, that finally fragments in several pieces while drying. The thickness of the drying paint layer can be controlled by the amount of solution placed in the tubes (D). The final crack patterns of the precipitated nail polish appears on the glass surface after 2-3 days of slow drying at room temperature. After carefully removing the graded tubes from the glass surface, it is possible to record digitally the fragmentation patterns produced in layers of different thickness. In Figure 1a these snapshots are presented for solution volumes of 2 – 7 ml. A first visual analysis of these pictures suggests that the number of fragments per unit area is decreasing as the layer thickness is increased, which means that the average fragment size is increasing with the layer thickness. Based on these snapshots the average fragment size is estimated by dividing the surface area with the total number of fragments. In Figure 1b we plot the results obtained for the average fragment size S, as a function of the layer thickness on double logarithmic scale. The fragment size S, is measured in units of Q, where Q is the total surface of the paint layer on the glass plate. In such view S is non-dimensional. Since we controlled the layer thickness by the amount of solvent placed in the tube, in Figure 1a we use D to quantify the layer thickness up to a proportionality constant. This data proves to be in good agreement with previously published results [9], confirming once again the claim that the average fragment size exhibits a power-law-type dependence as a function of the layer thickness. Our experiments suggest a scaling exponent of 1.72, in excellent agreement with previous results in the literature [9].

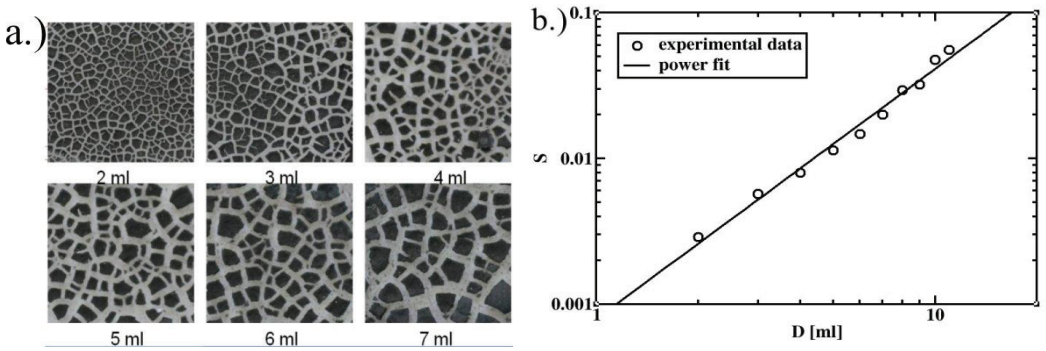


**FIGURE 1 a.** Experimentally obtained nail polish fragmentation patterns for different layer thicknesses controlled by the used solution volumes indicated on the figures. Visual observation: the thicker the layer the fewer fragments we get. b. Experimental results for the average fragment size scaling as a function of the layer thickness.

## III. THE THREE-DIMENSIONAL SPRING-BLOCK MODEL FOR QUASISTATIC FRAGMENTATION PROCESSES

The spring-block model family originates from the work of Burridge and Knopoff [14] who used this simple mechanical analogy to explain the power-law distribution of earthquakes' frequency as a function of their magnitudes [15]. Since then, many variants of the spring-block models have been developed to simulate various complex systems that exhibit self-organization and/or avalanche-like behavior [16].

In the most common two-dimensional version of the model identical blocks interconnected by a regular network of springs can slide on a frictional surface [9-13]. When one adopts this model to explain the drying of thin layers of wet granular material on a frictional surface, the blocks model the granules and the springs represents the capillary forces of the liquid between them [9, 10]. In order to introduce the possibility of fracture formation, each spring has a breaking threshold. The drying process builds a stress in the system, which is modeled by a recurrent increase of the spring constant values. This increase in the spring stress may lead to breaking and/or block slipping events. The relaxation of the stress by spring breaking or block slipping events can lead to avalanche-like processes, as it is illustrated in Figure 2b (see also [9-13]).

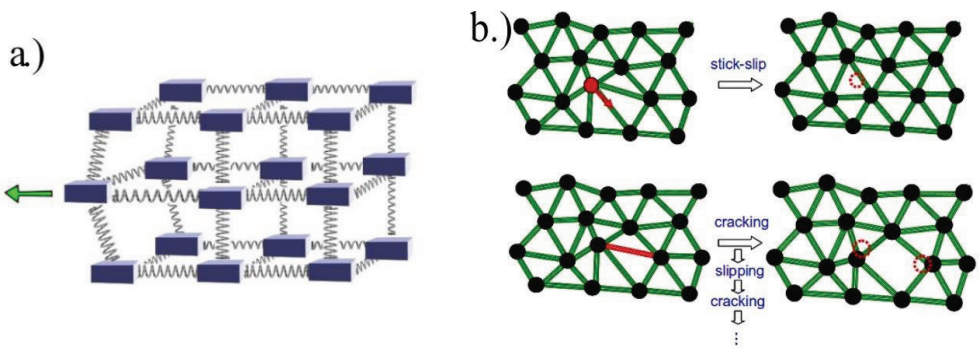


**FIGURE 2 a.** The 3D Spring-Block model uses blocks placed in a viscous environment. **b.** The dynamics of crack formation by stick-slip events.

In the three-dimensional (3D) approach considered here, the blocks are placed on the sites of random 3D lattice and the nearest neighbors detected by a Voronoi tessellation are connected by springs. This lattice is obtained by considering initially a regular 3D cubic lattice, and displacing the sites of this lattice in random direction and with a random length. A sketch of the 3D spring-block model for a uniform cubic lattice is illustrated in Figure 2a. Details for the construction of the random 3D lattice is given in the Appendix.

After the random 3D lattice is constructed, one can proceed to the simulation of the crack formation process. This part of the simulation program receives as input the previously built neighbor list and the relevant model parameters: the equilibrium length of springs l0, the spring breaking threshold Ft, the initial spring constant k0, the friction force Fs, and the time-length of a simulation steps dt.

The dynamics of the model consists of the following simulation steps, that are repeated until the final fragmented structure is obtained: (1) springs in which the spring force is greater than Ft are removed from the system; (2) each block is visited and resultant spring forces acting on them are calculated and compared with the slipping threshold Fs; (3) blocks on which the resultant force is bigger than Fs are moved with an overdamped dynamics into the direction of resultant force (at each simulation step only one block is moved, the one that has the maximal resultant force acting on it) (4) each simulation step is assumed to be a dynamical event of dt time-length; (5) the spring breaking and block-slipping steps (1 – 4) are repeated until no spring-breaking and block-slipping events can occur; (6) the new block positions are saved for visualization purposes; (7) the spring constant k is increased up to the smallest value, for which either one breaking or slipping event will occur. Simulations are done until all springs are broken. At each time-step, block positions and neighbor lists are updated.

The presented simulation steps (1)-(7) will lead to crack formation and propagation process in the spring-block system [9, 10, 12] (in a 2D topology this is sketched in Figure 2b). It has to be mentioned here that although we use time in the equations of motion of the MD type simulation, the simulation time is not realistic and cannot be compared to the experimental one. The reason for this is that the k spring constant values are varied in a discontinuous manner with largely different steps. However, our purpose here is not to give a realistic time-like dynamics, we are interested in generating the final and stable equilibrium crack patterns.

Graphical visualization of the dynamics is realized by generating a snapshot image series. Due to the fact that thin layers are studied, the most significant images are the two-dimensional top-view projections of the system (the XY plane as shown in the Figure 3). By studying the time series of these images the crack-line nucleation and propagation can be studied. Other two-dimensional projections are also available, i.e. XZ and YZ planes shown on the Fig. 3., but these projections will contain no valuable information, since the crack lines will not be visible in general cases.

The average relative size of the fragments S is computed using the last layer top-view projection of the system, dividing the total area of the system (considered to be 1) by the total number of fragments. This characteristic quantity is calculated for different layer thickness D.

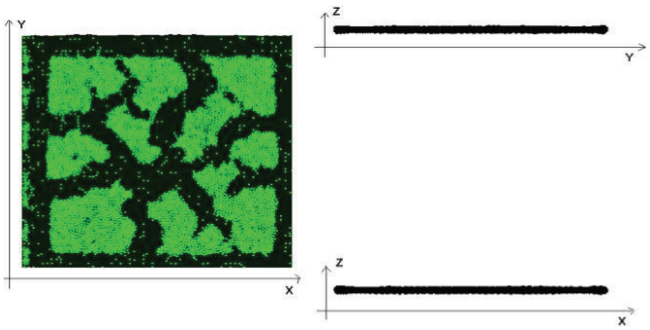


**FIG.3.** Various two-dimensional projections for the three-dimensional spring-block system. For thin layers the most useful projection is the one perpendicular to the plane of the layer (X-Y).

## IV. RESULTS AND DISCUSSION

First, in order to get realistic fragmentation patterns, the model has been tuned for the proper simulation parameters. Many parameter sets have been tested in case of smaller systems (of sizes 20x20x5) and it was found that the values Fs = 5, Ft = 20 and l0 = 8 produce patterns that visually resemble the ones obtained in our nail polish drying experiments. After we have visually confirmed the proper crack nucleation and propagation dynamics, we studied the variation of the average fragment size as a function of the simulated layers thickness. A first visual inspection of the simulated crack structures confirms the experimental finding that larger fragment sizes are obtained for thicker layers. Results obtained for systems of sizes (50x50) and (100x100) for different layer thicknesses, D is illustrated in Figure 4. One can also immediately observe that the simulated crack structures are qualitatively similar with the experimentally obtained ones (Fig. 5a). These images suggest also a variation of the average fragment size as a function of the layer thickness in agreement with the experiments.

In order to go beyond a simple visual comparison, the dependence of the average fragment size as a function of the layer thickness is computed. As it is shown on the graph from Figure 5b our simulation results reproduces successfully the power-law scaling of the average fragment size as a function of the layer thickness. Moreover, the 1.73 scaling exponent obtained from a linear regression is in excellent agreement with the 1.72 exponent found in the case of nail polish experiments.

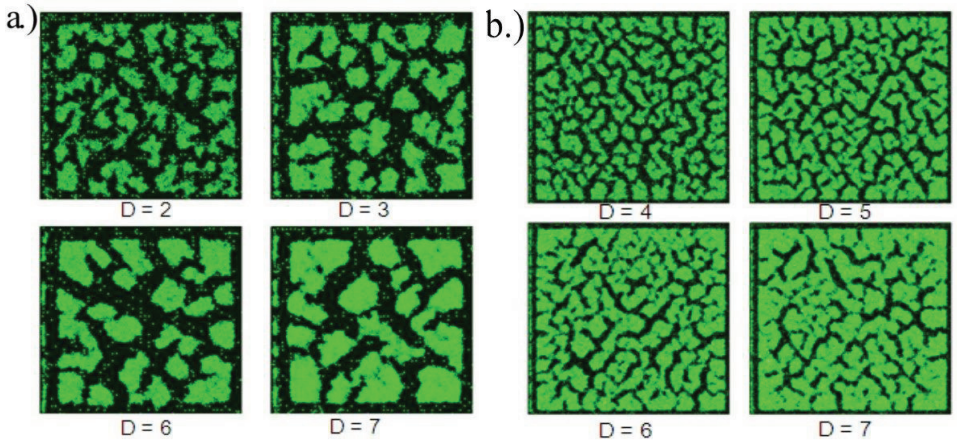


**FIGURE 4** Fragmentation patterns obtained in spring-block systems of different sizes. By increasing the thickness D of the layer larger and larger fragment sizes are obtained. a. Lattice size: 50x50, $F_s = 5$, $F_t = 20$, $l_0 = 7$.

b. Lattice size: 100x100, $F_s = 5$, $F_t = 20$, $l_0 = 8$.

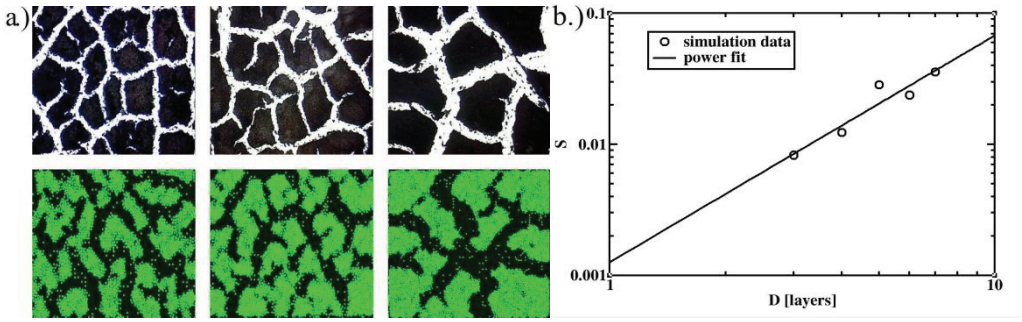


**FIGURE 5.** **a.** Visual comparison between the structures obtained by experiments (upper line) and computer simulations (bottom line). In both cases the layer thicknesses is proportionally increased from left to right. **b.** Simulation data showing the scaling of the average relative fragment size S as a function of the layer thickness D. Simulation parameters are: lattice size: 100x100, $F_s = 5$, $F_t = 20$, $l_0 = 8$.

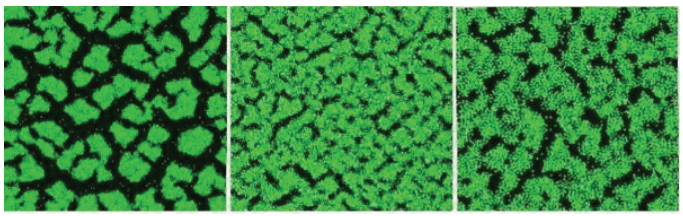

**FIGURE 6.** Qualitatively different structures obtained by the model for different parameter sets.

Additionally, we have also investigated qualitatively the fragmentation structures outside the initially fine-tuned parameter regime. Qualitatively different structures have been obtained and a few samples are illustrated in Figure 6. Regions fragmented with widely different cracks widths are observable on the left snapshot from Figure 6. In other parameter regimes more diffuse cracking patterns will arise as it is shown in the middle and right panels of the same figure. From these computational studies we have found that there is much more modelling potential in the elaborated model than it was initially expected. However, a more complete study of these parameter regimes are needed in order to fully understand the dynamics leading to these fascinating structures.

## CONCLUSIONS

Drying experiments of a special nail polish on glass surfaces and realistic 3D spring-block modeling have been performed in order to confirm the scaling of the average fragment size as a function of the layer thickness in the fragmentation process of thin layers of wet granular material dried on frictional surfaces. The novel 3D spring-block approach considered here yielded realistic crack structures and fragmentation dynamics. The universal scaling of the average fragment size as a function of the layer thickness was confirmed and the simulation yielded a scaling exponent in excellent agreement with the experimentally measured one.

## APPENDIX

**Construction of the random 3D lattice.** During the initialization procedure each block is labeled by an ordinal number. The coordinates of blocks are randomized, starting from a regular cubic lattice and taking into account that the blocks have a finite size and cannot overlap. We assume that the distance between any two blocks needs to be greater than the equilibrium distance of springs. These restrictions are satisfied starting from an ordered cubic lattice. During the randomization dynamics blocks are randomly selected, and a trial move is made in a random direction to a randomly selected small distance from the interval [0.01 $l_0$, 0.1 $l_0$]. If, according to the new position, the distance to any other block is greater or equal than $l_0$, then the move will be accepted. Else, the selected move is

rejected. These randomization steps are repeated many times, until the blocks are randomly mixed. The output of the randomization process will consist of a file, which includes the labels and the positions of each block. Once the positions are fixed we proceed to find the nearest neighbors. The nearest neighbor-finding algorithm uses the output file created by the previously described randomization process. The spring interaction between the blocks is realized on the network defined by the nearest neighbors. In order to construct this connection network the Voronoi tessellation or the Delaunay triangulation method is used. In our simulation code the Voronoi tessellation is realized first, based on the blocks as generator centers. The Voronoi cell around a center contains those points of the space that are closest to the same center [17]. Based on this tessellation, blocks that have common cell edges are considered as nearest neighbors and thus, will be connected by springs. The output of this initialization algorithm will be a file composed by rows for each block that contains its position and label, the number of neighbors and the neighboring blocks labels.

## ACKNOWLEDGEMENT

Financial support was provided by the research grant PNII-ID-PCE-2011-3-0348.

## REFERENCES

[1] M. Kaliske, H. Dal, R. Fleischhauer, C. Jenkel, C. Netzker, Characterization of fracture processes by continuum and discrete modeling, Comput. Mech. 50, 303 (2012).

[2] G. I. Kanel, A. M. Molodets, A. N. Dremin, Decomposition of cast trotyl in shock waves, Combustion, Explosion and Shock Waves 13, 772 (1977).

[3] Z. Rosenberg, D. Yaziv, S. J. Bless, Delayed failure in a shock-loaded silicon carbide, J. Appl.Phys. 58, 3249 (1985).

[4] N. S. Brar, S. J. Bless, Z. Rosenberg, Microcracks, spall and fracture in glass: A study using short pulsed laser shock waves, Appl. Phys.Lett. 59, 3396 (1991).

[5] H. D. Espinosa, Y. Xu, N. S. Brar, Experimental characterization of the dynamic failure behavior of mortar under impact loading, J. Am. Ceram.Soc. 80, 2074 (1997).

[6] J. J. Gilvarry, B. H. Bergstrom, Distribution of fragment size in repetitive fracture of brittle solids, J. Appl. Phys.,32, 400 (1961).

[7] T. Kadono, M. Arakawa, Break-up of shells under explosion and impact, Phys. Rev. E,65, 035107 (2002).

[8] B. Behera, F. Kun, S. McNamara, H. J. Herrmann, Crossover of the weighted mean fragment mass scaling in 2D brittle fragmentation, arXiv:cond-mat/0404057v1 (2004).

[9] K.T. Leung and Z. Neda, Physical Review Letter, vol. 85, 662 (2000)

[10] K.T. Leung and Z. Neda, Physical Review E, vol. 82, 046118 (2010)

[11] E-A Horvat, F. Jarai-Szabo, Y. Brechet, Z. Neda, Central European Journal of Physics, p. 926 (2012)

[12] K. T. Leung, L. Jozsa, M. Ravasz, Z. Neda, Nature 410, p. 166 (2001)

[13] F. Járai-Szabó, S. Aştilean and Z. Néda, Understanding self-assembled nanosphere patterns, Chem. Phys. Lett. 408, 241 (2005).

[14] R. Burridge and L. Knopoff, Bulletin of the Seismological Society of America, 57, 341 (1967)

[15] B. Gutenberg and C.F. Richter, Ann. Geophys., 9, 1 (1956)

[16] Z. Néda, F. Járai-Szabó, E. Káptalan and R. Mahnke, Control Engineering and Applied Informatics, 11, 3 (2009)

[17] F. Járai-Szabó, Z. Néda, On the size distribution of Poisson Voronoi cells, Physica A, 385, 518 (2007).